Three-dimensional fluctuation conductivity in superconducting single crystal K_3C_{60} and Rb_3C_{60}

X.-D. Xiang, J. G. Hou, Vincent H. Crespi, A. Zettl & Marvin L. Cohen

Department of Physics, University of California at Berkeley, and Materials Sciences Division, Lawrence Berkeley Laboratory, Berkeley, California 94720, USA

THE superconducting transition temperature, T_c, defines the point at which the free energies of the superconducting and normal states of a material become equal. Just above T_c, thermodynamic fluctuations produce small, transient regions of the superconducting state, giving rise to an anomalous increase in the normal-state conductivity known as paraconductivity. This situation is analogous to the fluctuating regions of correlated spins found near the Curie–Weiss transition in ferromagnets. Such fluctuations are of theoretical significance in that they provide a direct probe of critical phenomena in general, and a stringent test of scaling theories, which describe the approach to the critical point. Paraconductivity effects are strongly dependent on the dimensionality of the system, although for conventional superconductors, three-dimensional fluctuation conductivity has to our knowledge never been observed. Here we report the observation of pure, three-dimensional paraconductivity in single crystals of the recently discovered[1] superconductors K_3C_{60} and Rb_3C_{60}. In addition to probing the critical state near T_c, these measurements allow the indirect determination of the residual, normal-state resistivity.

High-quality single-crystal specimens of K_3C_{60} and Rb_3C_{60} were prepared by doping vapour-transport-grown C_{60} crystals with alkali metals. The synthesis followed a method similar to that described previously[2] for K_3C_{60}. We used the standard in-line four-probe contact configuration and kept the d.c. probing current small (10–100 μA) to minimize Joule heating effects.

The insets to Fig. 1*a* and *b* show, for K_3C_{60} and Rb_3C_{60}, respectively, the (normalized) resistivity $\rho(T)$ as a function of temperature over an extended temperature range. As demonstrated previously[2] for K_3C_{60}, the temperature dependence of ρ for Rb_3C_{60} is metallic. This behaviour is in contrast to the nonmetallic temperature dependence of $\rho(T)$ found for Rb-doped C_{60} when C_{60} crystals grown from a CS_2 solution were used[3]. Although the origin of this discrepancy is unknown, a nonmetallic $\rho(T)$ may result from incomplete doping or an impure host crystal. Our resistively determined T_c values (transition midpoint) for K_3C_{60} and Rb_3C_{60} are 19.8 K and 30.2 K, respectively. We note that the overall functional form for $\rho(T)$, except at temperatures below 50 K, is similar for K_3C_{60} and Rb_3C_{60}. The temperature dependence of $\rho(T)$ is reproducible over many samples in both cases.

Figure 1*a* and *b* also shows $\rho(T)$ for K_3C_{60} and Rb_3C_{60} in greater detail near T_c (the temperature scale has been normalized to T_c in each case). Just above T_c, the resistivity for both materials deviates from its normal-state behaviour before dropping precipitously at T_c. We associate this deviation with superconducting fluctuations. It should be recognized that identification of fluctuation effects of small magnitude requires data with a high signal-to-noise ratio. In an earlier investigation[2] of the resistivity of K_3C_{60}, fluctuation effects near T_c were not resolved because of large scatter in the data.

The paraconductivity, σ', is obtained by subtracting the extrapolated normal-state conductivity σ_n from the measured conductivity. To establish an appropriate baseline for the paraconductivity, we have tried various power-law extrapolations using the temperature range $1.4T_c < T < 2T_c$ to establish fitting parameters for the extrapolation. For both materials, a linear $-T$ curve provides an adequate fit (solid line in Fig. 1*a* and *b*). In K_3C_{60}, a T^5 curve (dashed line in Fig. 1*a*) provides a slightly better fit at higher temperatures ($T \approx 60$ K). But as shown in Fig. 1*a*, the difference between the two extrapolations is small in the relevant temperature range near T_c, and both are consistent with ρ measured near T_c at high magnetic field (also shown in Fig. 1*a*). Without further physical basis, in our analysis we shall use the T^5 extrapolation for K_3C_{60} and the linear $-T$ extrapolation for Rb_3C_{60}. Our conclusions of three-dimensional paraconductivity are not sensitive to which extrapolation is used. The baseline choice does affect the determined numerical value of the residual normal-state resistivity (see below), but different

reasonable extrapolations lead to resistivities all within 20% of one another.

As first derived by Aslamazov and Larkin (AL)[4], the excess conductivity σ' is given by[5]

$$\sigma'_{AL} \sim t^{-(4-D)/2} \quad (1)$$

where D is the dimensionality of the specimen and t is the reduced temperature defined by $t = (T - T_c)/T_c$. This AL term is known as the regular fluctuation conductivity, which is due to the direct acceleration of the fluctuation-induced superconducting pairs of quasiparticles. In addition to the AL term, Maki[6] and Thompson[7] (MT) have derived another contribution known as the anomalous fluctuation conductivity. The MT term results from the scattering of the normal quasiparticles by the superconducting fluctuations and is small when 'pair-breaking' effects are large.[8] In three dimensions, the excess conductivity may be expressed as[8]

$$\sigma'_{3D} = \sigma'_{AL} + \sigma'_{MT} = \sigma_{exc}\left[t^{-1/2} + \frac{4}{t^{1/2} + \delta^{1/2}}\right] \quad (2)$$

where δ is a pair-breaking parameter. The first term on the right is the AL term, and the second is the MT term. σ_{exc} is a prefactor to be defined below.

Figure 2*a* and *b* shows on log-log plots the experimentally determined σ' against T/T_c for K_3C_{60} and Rb_3C_{60}. The insets show log-log plots of σ' against t for the same data sets. The paraconductivity data for K_3C_{60} and Rb_3C_{60} can be well accounted for by assuming an effective dimensionality $D = 3$. For K_3C_{60} (Fig. 2*a*), we find that including a MT contribution improves the fit (although the AL term dominates). From our best fit, we obtain a pair-breaking parameter $\delta \approx 0.58$ for K_3C_{60}. For Rb_3C_{60} (Fig. 2*b*), we find that a good fit is obtained only if the MT term is negligible, which implies a large δ. This is consistent with Rb_3C_{60} having a stronger electron-phonon coupling constant (resulting in a higher T_c) than K_3C_{60} (ref. 9). Only for $D = 3$ do we obtain good fits to the paraconductivity data of K_3C_{60} and Rb_3C_{60}. The inset to Fig. 2*b* shows how the data of Rb_3C_{60} compare to paraconductivity fits with $D = 1$ and $D = 2$ in addition to $D = 3$.

We observe no evidence for granular superconductivity. The coherence volume of the superconducting order parameter grows as the temperature approaches T_c unless limited by reduced dimensionality. For a granular superconductor with grain size of L, the functional form of the excess conductivity crosses over from three-dimensional behaviour to zero-dimensional behaviour when the Ginzburg-Landau coherence length $\xi(T)$ exceeds $L/3$ as T approaches T_c (ref. 10). In the presence of 0-D crossover, the data of Fig. 2*a* and *b* would deviate upwards away from the theoretical curves based on 3-D fluctuations with decreasing reduced temperature t, and there would be a region of steeper slope (-2) at small t. Such behaviour is not observed for either K_3C_{60} or Rb_3C_{60} (see insets to Fig. 2*a* and *b*). The absence of a 0-D crossover down to $t \approx 0.0005$ in our data gives a lower limit for the domain size of about 0.6 μm. This dimension is at least 100 times larger than the measured values of $\xi(0)$[11,12], and therefore guarantees that physical parameters measured on these samples reflect intrinsic properties.

An important parameter in describing electronic transport in K_3C_{60} and Rb_3C_{60} is the absolute magnitude of the resistivity. Because of uncertainties in sample dimensions, contact position and current distribution profiles (if a van der Pauw configuration is applied), it is difficult to make an accurate direct determination of the resistivity. Experimentally, we observe identical normalized fluctuation resistivity curves (therefore, identical σ'/σ_n) in different samples with somewhat different estimates of $\rho(0)$ based on direct measurements. However, the normal-state conductivity σ_n may be determined indirectly through the measured normalized conductivity (σ'/σ_n), because the excess conductivity prefactor σ_{exc} is related to the independently determined coherence length $\xi(0)$ by

$$\sigma_{exc} = \frac{e^2}{32\hbar\xi(0)} \quad (3)$$

Using equation (2) together with the experimentally determined values $(\sigma_{exc}/\sigma_n)_K \approx 2 \times 10^3$, $(\sigma_{exc}/\sigma_n)_{Rb} \approx 7.3 \times 10^{-3}$, $\xi(0)_K \approx 45$ Å (ref. 11) and $\xi(0)_{Rb} \approx 24$ Å (ref. 12), we obtain the zero-temperature residual normal-state resistivities $\rho(0)_K \approx 0.12$ mΩ cm and $\rho(0)_{Rb} \approx 0.23$ mΩ cm, where the subscripts K and Rb represent K_3C_{60} and Rb_3C_{60}, respectively. The different extrapolations of the normal-state resistivity produce an uncertainty of about ±20% in $\rho(0)$. The resistivity values are reasonably consistent with our most reliable direct measurement on K_3C_{60} (~0.5 mΩ cm) and with infrared studies[13] on Rb_3C_{60} (~0.4 mΩ cm). The results also agree with our theoretical calculation[11] ($\rho(0)_K \approx 0.2$ mΩ cm) based on H_{c2} measurements and a theoretical calculation[4] ($\rho(0)_K \approx \rho(0)_{Rb} \approx 0.39$ mΩ cm) in which a maximum disorder (defined as equal distribution of two possible orientations of C_{60} in a face-centred cubic structure) was assumed for both K_3C_{60} and Rb_3C_{60}. Our results suggest that Rb_3C_{60} may have a more C_{60} orientational disorder than K_3C_{60}.

As this is, to our knowledge, the first observation of pure 3-D paraconductivity in any isotropic superconductor, it seems appropriate to address the difficulty of observing similar

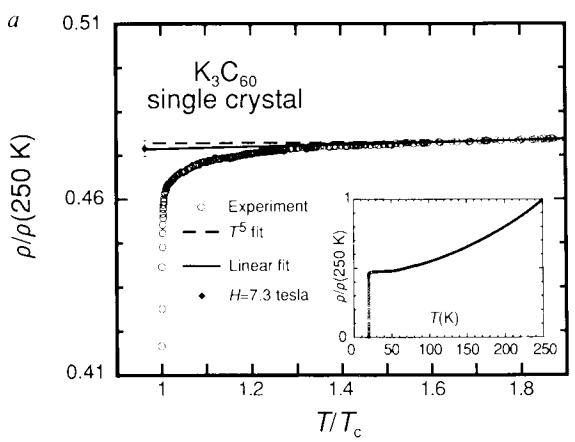

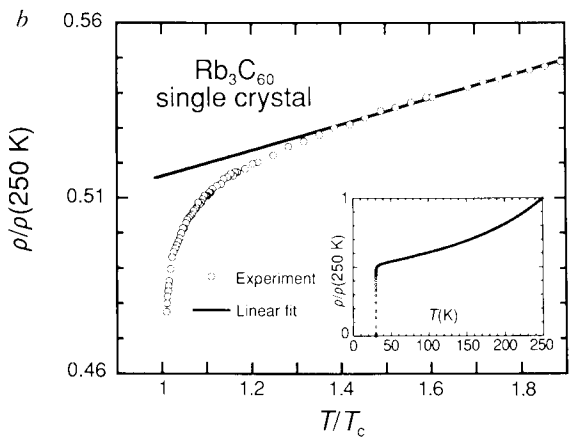

FIG. 1 Normalized resistivities as a function of T/T_c for K_3C_{60} (*a*) and Rb_3C_{60}(*b*). Circles are experimental data and solid lines are linear extrapolations to the normal-state resistivity. For K_3C_{60}, a T^5 extrapolation is also shown along with a high-magnetic-field resistivity point. Insets: normalized resitivities against temperature for K_3C_{60} (*a*) and Rb_3C_{60}(*b*).

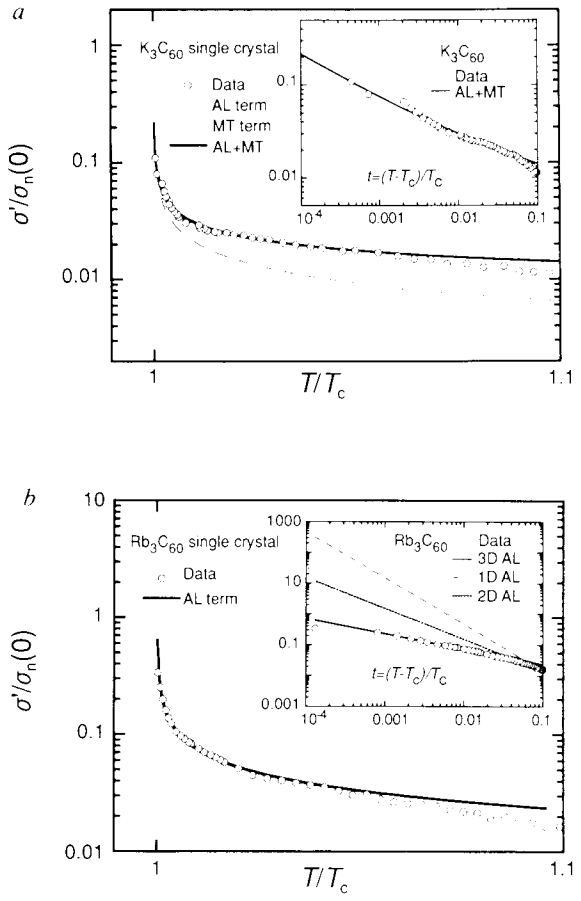

FIG. 2 Log–log plots of normalized fluctuation conductivities against T/T_c for K_3C_{60}(*a*) and Rb_3C_{60} (*b*). Insets: log–log plots of normalized fluctuation conductivities against reduced temperature $t=(T-T_c)/T_c$ for K_3C_{60} (*a*) and Rb_3C_{60} (*b*).

behaviour in other materials (most conventional superconductors are, of course, three-dimensional). For conventional 3-D superconductors, the fractional change in normal conductivity $\sigma'/\sigma_n \approx (kT_c/E_F)(1/k_F l)(T/(T-T_c))^{1/2}$ is of order of $10^{-7}(T/(T-T_c))^{1/2}$, too small to be observable in any meaningful temperature interval above T_c. Here E_F is the Fermi energy, k_F the Fermi wave vector, and l the mean free path. To observe 3-D fluctuation conductivity, large concentrations of impurities or defects have to be induced, and these are usually accompanied by granularity or reduced dimensionality. For anisotropic-layered high-T_c materials, the situation is more complicated. Paraconductivity has been reported for many different compounds in various forms, but no consensus about the dimensionality in these materials has been reached[8,15]. In the fullerene-based superconductors, the intrinsic orientational disorder (leading to a relatively high intrinsic resistivity or short mean free path), short coherence length and high T_c together greatly extend the useful temperature range for measurement of the fluctuations and allow direct observation of the fluctuation phenomena in pure single crystals. Our results demonstrate that these systems are genuinely 3-D superconductors as opposed to lower-dimensional or granular superconductors. □

Received 17 August; accepted 21 November 1992.

1. Haddon, R. C. *et al. Nature* **350,** 320 (1991).
2. Xiang, X.-D. *et al. Science* **256,** 1190 (1992).
3. Ogata, H. *et al. Jpn J. appl. Phys.* **31,** L166 (1992).
4. Aslamasov, L. G. & Larkin, A. I. *Phys. Lett.* A**26,** 238 (1968).
5. Skocpal, W. J. & Tinkham, M. *Rep. Prog. Phys.* **38,** 1049 (1975).
6. Maki, K. *Prog. theor. Phys.* **39,** 887 (1968); **40,** 193 (1968).
7. Thompson, R. S. *Phys. Rev.* B**1,** 327 (1970); *Physica* **55,** 296 (1971).
8. Maki, K. & Thompson, R. S. *Phys. Rev.* B**39,** 2767 (1989).
9. Appel, J. *Phys. Rev. Lett.* **21,** 1164 (1968).
10. Schmidt, H. *Z. Phys.* **216,** 336 (1968).
11. Hou, J. G., Crespi, V. H. Xiang, X.-D., Zettl, A. & Cohen, M. L. *Phys. Rev. Lett.* (submitted).
12. Sparn, G. *et al. Phys. Rev. Lett.* **68,** 1228 (1991).
13. Rotter, L. D. *et al. Nature* **355,** 532 (1992).
14. Gelfand, M. P. & Lu, J. P. *Phys. Rev.* B**46,** 4367 (1992).
15. Reggiani, L. & Vaglio, R. *Phys. Rev.* B**44,** 9541 (1991).

ACKNOWLEDGEMENTS. We thank W. A. Vareka, G. Briceno and B. Burk for technical assistance. This research was supported by the NSF and by the Office of Energy Research, Office of Basic Energy Sciences, Materials Sciences Division of U.S. Department of Energy. V.H.C. was supported by a National Defense Science and Engineering Graduate Fellowship.